Lithostratigraphy of the Naros Granite (Komsberg Suite), South Africa and Namibia

P.H. Macey and R.J. Thomas
Council for Geoscience, P.O. Box 572, Bellville, 7535, South Africa
e-mail: pmacey@geoscience.org.za; bthomas@geoscience.org.za

H.P. Smith
Council for Geoscience, P.O. Box 5347, Walmer, Gqeberha, 6065, South Africa
e-mail: hsmith@geoscience.org.za

D. Frei
Department of Earth Sciences, University of the Western Cape, Private Bag X17, Bellville 7535, South Africa
Central Analytical Facility, Stellenbosch University, Private Bag X1, Matieland 7602, South Africa
e-mail: dfrei@uwc.ac.za

P.J. le Roux
Department of Geological Sciences, University of Cape Town, South Africa
e-mail: petrus.leroux@uct.ac.za

Abstract

The Naros Granite occurs as a large, northwest-trending ovoid batholith roughly 30 km long and 15 km wide straddling the Orange River border between South Africa and Namibia, 25 km northeast of Onseepkans. It consists mainly of a leucocratic to mesocratic grey, coarse-grained equigranular hornblende-biotite granite-granodiorite that is locally mildly feldspar porphyritic. Small, ovoid mafic autoliths are common and characteristic of the Naros Granite. The composition of the unit varies from granite to granodiorite with a minor leucogranitic phase observed along the southern margin of the batholith. Hornblende and biotite are ubiquitous mafic minerals but small amounts of orthopyroxene occur locally. The Naros Granite has yielded tightly-constrained U-Pb zircon ages between 1114 Ma and 1101 Ma.

The Naros Granite is generally unfoliated to weakly deformed with only localised shearing along contacts with the surrounding country rocks giving rise to orthogneissic fabrics. It has an intermediate to felsic composition (mean SiO_2: 63.9 ± 2.2 wt.%) and is strongly metaluminous. This, together with its biotite-hornblende ± orthopyroxene mineral assemblage and the abundance of mafic autoliths, suggests it is an I-type granitoid, with the source magma produced by partial melting of older igneous rocks that had not undergone any significant chemical weathering.

The Naros Granite is the youngest and most evolved member of the ~1.11 Ga Komsberg Suite, a collection of late- to post-tectonic I-type metaluminous, intermediate to felsic, biotite ± hornblende granitoids and their charnockitic equivalents that have intruded the older pre-tectonic gneisses of the Kakamas Domain of the Namaqua Metamorphic Sector.

Introduction

The late-tectonic Naros Granite, a member of the Komsberg Suite, occurs as an ovoid body that intruded the older pre-tectonic gneisses at the base of the high T-low P Kakamas Domain in the Namaqua Sector of the Namaqua-Natal Metamorphic Province (NNMP, Cornell et al., 2006; Macey et al., 2018; Figure 1). Toogood (1976) first recognised and mapped the granite in southern Namibia where he named it the "Naros granitoid formation" after the farm *Naros 76*. Du Plessis (1979, 1986) named the unit the "Naros Granite" in the adjacent area south of the Orange River and this name was used on subsequent 1:50 000 and 1:250 000 scale geological survey maps in South Africa and Namibia (Moen and Toogood, 2007; Macey et al., 2015).

Type Area

The Naros Granite is well exposed along the Orange River and the adjacent farming areas. The original type area for the unit, as described by Toogood (1976), is on the farm *Naros 76* in southern Namibia (28°37'54"S; 19°29'47"E). Good exposures can be easily reached along the tarred road leading to the Keboes Fruit Farm located east of Onseepkans which is identified here as the type area in South Africa (*Styr-Kraal 81*; 28°43'27"S; 19°28'54"E; Figure 2). The very minor "leucogranite' phase can also be observed on the farm *Styr-Kraal 81* (28°44'16"S; 19°29'5"E; Figure 2).

Stratigraphic position and age

The Naros Granite is the youngest member of the 1125 to 11005 Ma Komsberg Suite (Macey et al., 2015), a collection of late- to post-tectonic I-type metaluminous, intermediate to felsic, biotite ± hornblende granitoids and their charnockitic equivalents that have intruded the older pre-tectonic gneisses of the Kakamas Domain between Riemvasmaak and Grünau (Figure 1; Macey et al., 2015, 2018; Abrahams and Macey, 2020). The Naros Granite intrudes, and contains xenoliths of, older strongly foliated gneisses dated between about 1 220 and 1 140 Ma (Moen and Toogood, 2007; Macey et al., 2015; Bial et al., 2015; Groenewald and Macey, 2020; Doggart et al., 2021).

Two samples of the Naros Granite, collected from just north of the Orange River, were dated during this study (Figure 2). Sample PM14072 is from the eastern parts of the Naros batholith near the border of *Naros 76* and *Ondermatjie 75* farms (28°32'12"S; 19°31'39"E). The medium- to coarse-grained equigranular granite contained tabular to elongate subhedral zircons (100 to 200 µm) with blunt rounded terminations and no internal zonation. Most of the zircons are low in uranium, but with thin high-U rims, some of which were wide enough to be analysed. Of the 22 analyses carried out, all 11 concordant core-rim pairs gave indistinguishable ages and together yielded a precise concordia age of 1 114 ± 8 Ma (MSWD = 0.36, Probability = 0.99; Figure 3) which is considered the age of intrusion. Sample RT14001 was collected along the boundary of *Naros 76* and *Beenbreek 152* farms (28°38'59"S; 19°29'9"E). Twenty-four spots were analysed of which the most concordant 14 provided a concordia age of 1 113 ± 6 Ma (MSWD = 0.35, Probability = 0.99; Figure 3). No inherited zircons were identified in either sample. These new ages are statistically identical to the previously published date of Du Plessis (1986) who obtained a U-Pb upper intercept age of 1 107 Ma and by Bial et al. (2015) who report upper intercept ages of 1 109 ± 11 and 1 101 ± 6 Ma. The dates overlap with those of other members of the Komsberg Suite (Macey et al., 2015, 2018; Abrahams and Macey, 2020).

The Komsberg Suite is similar in mineralogy, geochemistry and relative tectonic timing to the late- to post-tectonic granitoids of the Keimoes Suite that intrude the southeast Kakamas Domain. However, The SACS Task Group for the Mesoproterozoic resolved to keep the two suites separate as they are geographically distinct (~50 km apart) and the Keimoes Suite has a larger spread of ages (1 113 to 1 078 Ma; Cornell et al., 2012; Bailie et al., 2017).

Geographic distribution, form and size

The Naros Granite occurs as a single, north-northwest–trending oval batholith, approximately 15 x 30 km in size, along the western margin of the Kakamas Domain, about 25 km northeast of Onseepkans (Figure 1). Itin stretches from *Styr-Kraal 81* farm in South Africa to *Ondermatje 75* in Namibia (Figures 1 and 2; Du Plessis, 1979, 1986; Moen and Toogood, 2007; Macey et al., 2015).

Geological description

Basic concept and unifying features

For the most part, the Naros is a grey, coarse-grained, mostly unfoliated, equigranular hornblende-biotite granite/ granodiorite which is easily distinguishable from the surrounding pre-tectonic orange-weathering augen orthogneisses and the other, generally megacrystic, members of the Komsberg Suite. Abundant small mafic autoliths are very characteristic. It locally grades into minor leucogranitic (*2 on Figure 2) and feldspar-porphyritic varieties in the southern parts of the batholith (Figures 4 and 5).

The Naros Granite forms rusty-grey coloured, well-jointed, rounded boulder tors groups of tors which in places rise up to 20 m above the surrounding sandy plains (Toogood, 1976; Macey et al., 2015; Figures 4a and 4b).

Lithology

The mineralogical composition of the unit typically grades from granite (*sensu stricto*) to granodiorite, with monzogranite (roughly equal K-feldspar and plagioclase abundance) being most prevalent. All rocks are quartz-rich (25 to 35 volume %). K-feldspar (30 to 43%) is invariably unaltered microcline string microperthite, while plagioclase (20 to 32%; ~An_{40}) is slightly sericitised. Typically, both greenish brown or green hornblende and highly pleochroic brown biotite occur in equal modal amounts, but some rocks contain biotite alone (total mafic

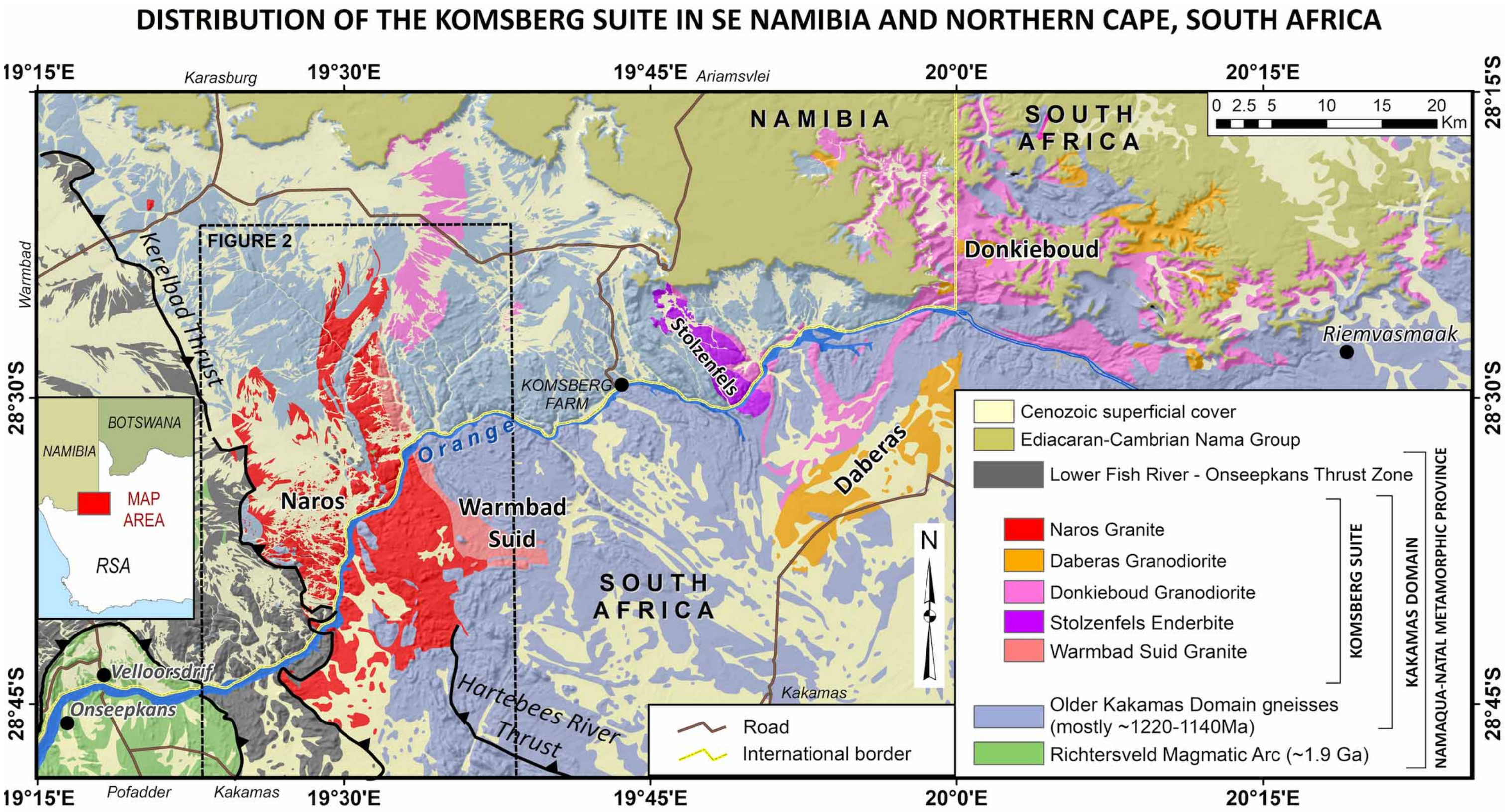

Figure 1. *Distribution of the Komsberg Suite (of which the Naros Granite is a component) in the Orange River border region between South Africa and Namibia. Compiled from the 1:250 000 scale geological maps of Moen (1988), Moen and Toogood (2007) and the 1:50 000 geological maps of Macey et al. (2015). Dashed black line indicates the map of the type area as shown in Figure 2.*

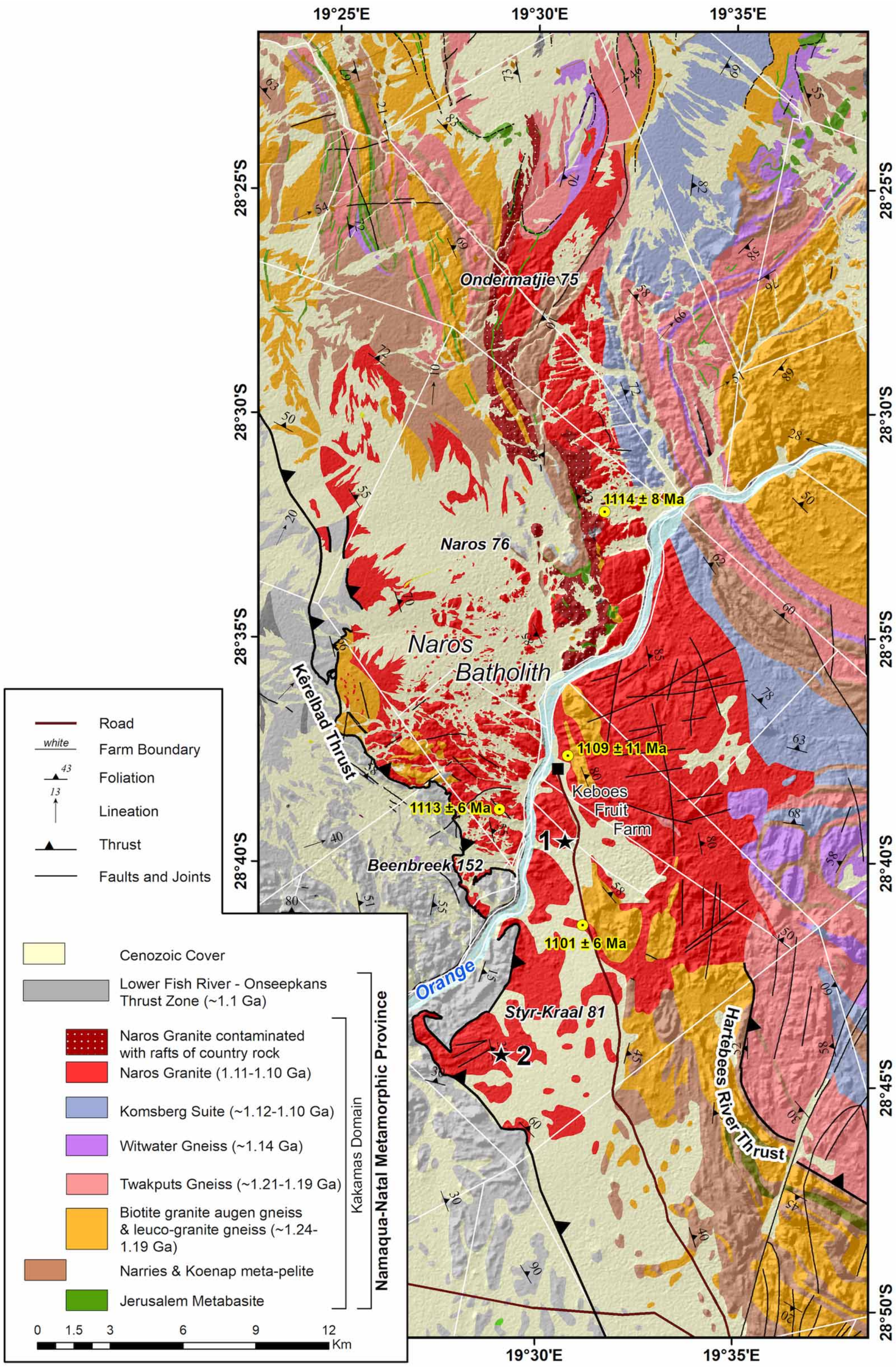

Figure 2. *Geological map of the Naros Granite batholith showing the type area of the typical homogenous hornblende-biotite granite on Styr-Kraal 81 (*1). The *2 indicates the location of the leucocratic phase of the Naros Granite. Compiled from the 1:250 000 scale geological map of Onseepkans by Moen and Toogood (2007), the 1:50 000 geological maps of Macey et.al. (2015) and the 1:50 000 geological maps of Onseepkans and Oupvlakte by Smith and Macey (2018).*

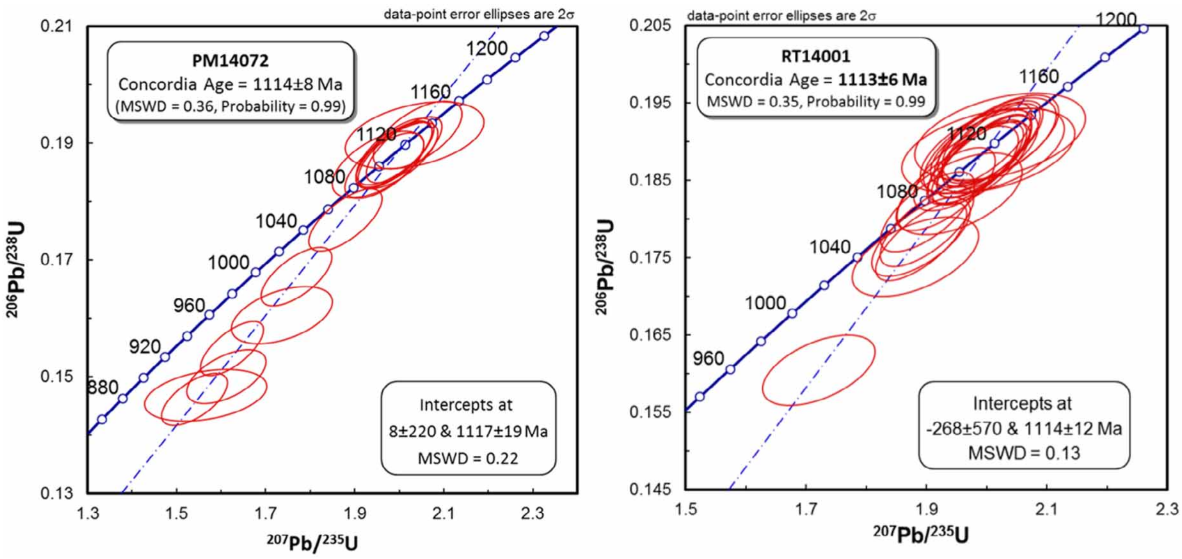

Figure 3. *Wetherill concordia diagrams showing LA-ICPMS zircon U-Pb data for two samples of Naros Granite.*

minerals ~10 to 20%). The two minerals tend to occur together in mafic aggregates. Hornblende is notably poikilitic in some samples. All thin sections show abundant accessory minerals including titanite, apatite and zircon ± allanite ± opaque minerals (Du Plessis, 1986; Macey et.al., 2015). Some samples contain additional minor orthopyroxene but these samples have the same appearance as the rest of the Naros Granite and do not have the typical olive brown colour of charnockite.

The Naros Granite is mostly coarse-grained (5 to 8 mm) and equigranular but becomes finer-grained along its eastern margin and is locally sparsely K-feldspar-porphyritic (10 to 20 mm ovoid, anhedral phenocrysts) along the southern margin in South Africa (Figure 4; Macey et al., 2015; Moen and Toogood, 2007).

Du Plessis (1986) mapped several small (~0 to 50 m) bodies of coarse-grained leucogranite in the southern parts of the pluton which he named the "leucophase" of the Naros Granite (Figure 4d). The mildly foliated leucogranite consists of microcline microperthite (40 to 50%), quartz (30 to 37%) and plagioclase (20 to 30%) together with minor / accessory biotite, hornblende, magnetite, titanite, allanite, zircon and apatite (Du Plessis, 1986).

Inclusions

The Naros Granite is characterised by the common presence of unfoliated mafic autoliths (Figures 4c and 4d) varying in size from the most typical 8 to 15 cm up to 30 cm in size. The autoliths often contain prominent small (2 mm), white plagioclase crystals. In thin section, the coarse-grained mafic autoliths have a gabbroic composition and are comprised of green hornblende (65%), pale green clinopyroxene (20%), plagioclase (15%) with accessory apatite and rare titanite and opaque minerals.

Xenoliths of the surrounding country rocks (Figure 5c) are prevalent near the margins of the Naros batholith, especially in

Figure 4.(a) *and. **(b)**. The Naros Granite weathers to boulder-tors (Naros 91 Farm); **(c)** and **(d)** Typical examples of the unfoliated, coarse-grained equigranular hornblende-biotite granite with mafic autoliths.*

***Figure 5**. (**a**) and (**b**). Weakly K-feldspar porphyritic examples of the Naros Granite; (**c**) A xenolith of older leucogneiss hosted in weakly porphyritic Naros Granite; (**d**) Leucogranite phase of the Naros Granite*

the northeast where Toogood (1976) described a zone of smaller sills of Naros Granite intimately associated with older rocks. He mapped this inclusion-rich part of the batholith as "Contaminated Naros" (Figure 2). Macey et al. (2015) also recognised this zone and reported tabular rafts of country rock (including Austerlitz leucogranite gneiss, Narries metapelite and Twakputs garnet-augen gneiss) ranging in width from 10 to 250 m. Xenoliths of leucogranite gneiss (Gemsbokvlakte Gneiss) were also observed on *Styr-Kraal 81* near the southern margin of the batholith where the rafts reach up to 100 m in size.

Structure

The Naros Granite is generally massive (Figures 4 and 5) but a poorly developed gneissic foliation that parallels the regional tectonic fabric in the surrounding intensely foliated country rocks is locally apparent. This late-tectonic fabric is defined by weak to moderate alignment of flattened quartz and feldspar and decussate biotite. Along the westernmost boundary of the batholith, the Naros Granite becomes more strongly deformed with the intensity of foliation increasing progressively towards the basal Kêrelbad Thrust of the Kakamas Domain (Figures 2 and 6). Low-angle sheets of foliated and lineated Naros Granite occur tectonically interleaved with older gneisses along the Kêrelbad Thrust (Macey et al., 2015; Smith and Macey, in prep). In contrast, the Naros Granite intrudes across Hartebees River Thrust thus providing a minimum age for this structure which forms the major tectonic boundary between the Kakamas Domain and the Bushmanland Subprovince.

Narrow (m-scale), discrete late-Namaqua sub-vertical ductile shear zones sporadically transect the Naros Granite. The granite is well jointed with regular joint sets displayed in outcrop.

Boundaries

As described above, the eastern margin of the Naros batholith is characterised by a wide zone of intrusive migmatite with concordant granite sills intruded along the regional foliation planes in the layered host rocks. The western margin of the batholith is truncated by the Kêrelbad Thrust, the basal tectonic boundary of the Kakamas Domain. The contact between the main granite phase and the minor leucogranite phase is a gradational zone a few metres wide characterised by biotite- and quartz-feldspar schlieren (Du Plessis, 1986).

Subdivision and lateral variations

The Naros Granite is mostly homogenous in composition and texture and, except for the minor leucogranite phase, cannot be further subdivided.

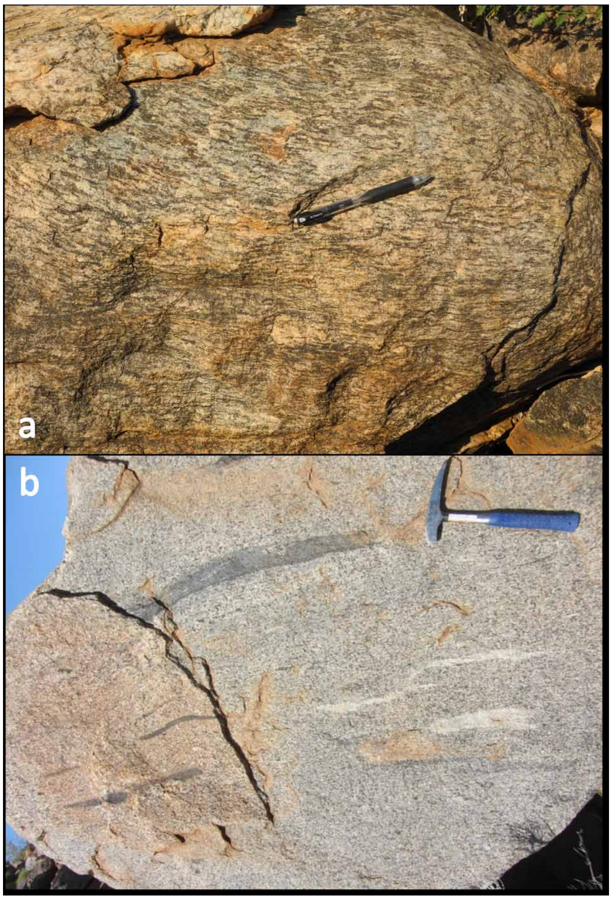

Figure 6. *(**a**) Foliated Naros Granite in the Kerebad Thrust zone at the base of the Kakamas Domain. Note the stretched out mafic autoliths and felsic xenoliths in (**b**).*

Geochemistry and petrogenesis

The geochemistry of 11 samples analysed during this study are reported here (Table 1) and plotted together with 25 samples from Du Plessis (1986) and Bial et al. (2015). Analyses of other members of the Komsberg Suite are also shown for comparison (data from Du Plessis, 1986; Macey et al., 2015, 2018; Abrahams and Macey, 2020).

The Naros Granite samples presented in this study show a range in SiO_2 concentrations from 65 to 72 wt% (mean: 67.7 ± 1.9 wt%; Table 1) and classify mostly in the subalkaline granodiorite field on the total alkali versus silica diagram (Cox et.al., 1979; Figure 7a), but a few samples classify as granite and alkali granite. Using calculated mesonormative mineral compositions, the samples classify as monzogranite and granodiorite on the Streckeisen and le Maitre (1979) Q-A-P diagram. The disparity between the petrographic (as granite) and geochemical (as granodiorite) classifications is due to the perthitic nature of the K-feldspar. The Naros Granite is mostly strongly metaluminous with an average alumina saturation index values of 0.9 (Figure 7b; Shand, 1943).

The granitoids of the Komsberg Suite show consistent major and trace element trends (Figures 8 and 9), suggesting that they represent fractionated variants of the same source magma. Bivariate Harker diagrams show an overall trend of decreasing CaO, Fe_2O_{3TOT}, TiO_2, Al_2O_3 and MgO with increasing SiO_2, whereas Na_2O concentrations are fairly constant. The trace element patterns of the Naros Granite, as shown on the normalised spider diagrams, are consistent with the rest of the Komsberg Suite (Figure 9a) with enrichment in large ion lithophile and high field strength elements (e.g. Sc, La, Ce, Y, Yb, ΣREE and Th). Rb is mildly elevated and Sr is depleted relative to average granite and the rest of the Komsberg Suite.

The Naros Granite samples have very high total rare earth element (REE) concentrations (mean ΣREE = 1 118 ± 148 ppm), significantly higher than average granite and average continental crust (Chayes, 1985; Taylor and McLennan, 1985). They display moderate to strong light REE enrichment patterns (La/Yb_N between 8.2 and 14.6, mean: 10.7 ± 2.1) and moderate Eu_N anomalies (0.49 to 0.62, mean: 0.58 ± 0.05) consistent with the

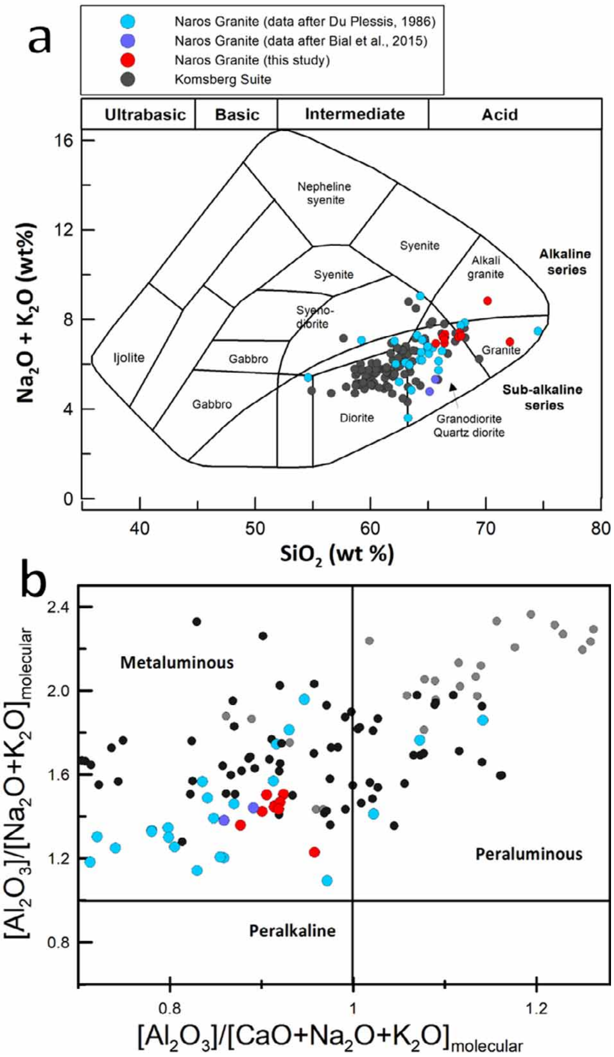

Figure 7. *(**a**) Total alkali versus silica classification (Cox et al., 1979) for the Naros Granite relative to the rest of the Komsberg Suite; (**b**) The Naros Granite plots in the metaluminous field of the alumina saturation diagram (Shand, 1943).*

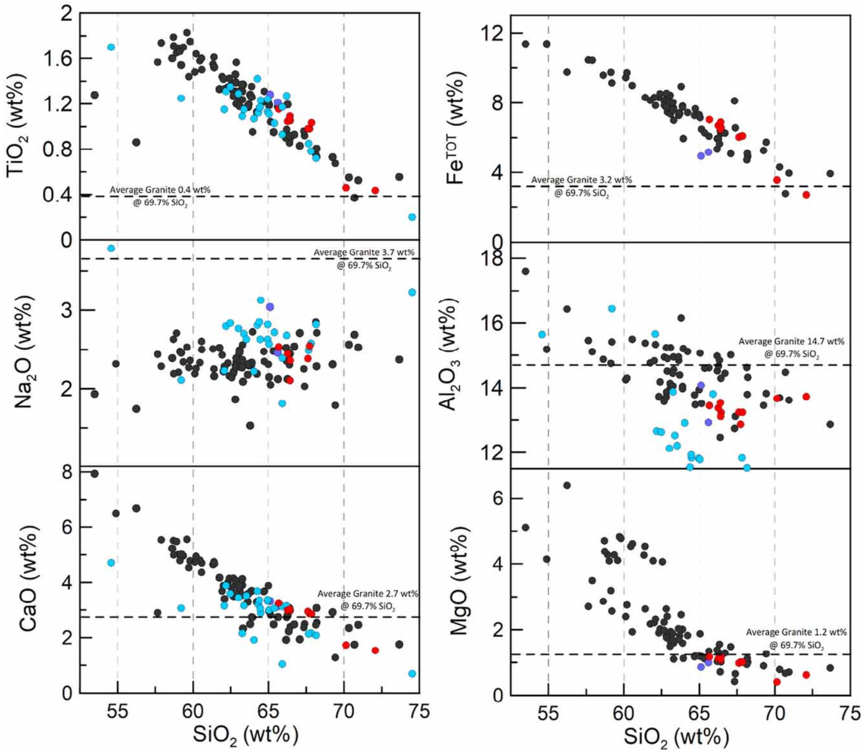

Figure 8. *Harker bivariate major element diagrams for the Naros Granite and the other members of the Komsberg Suite (symbols as for Figure 6a).*

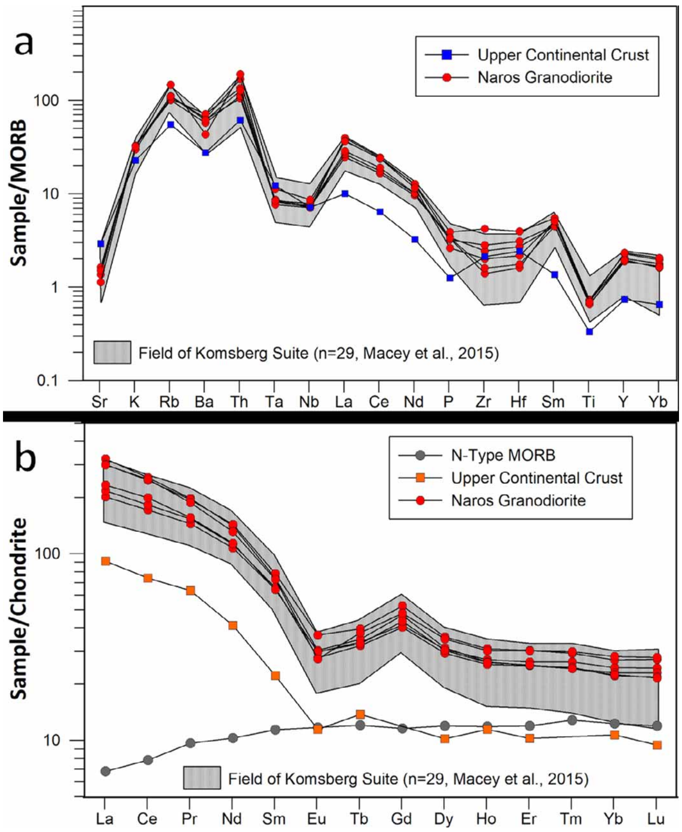

Figure 9. *Normalised trace element **(a)** and rare earth element **(b)** diagrams of the Naros Granite (in red) relative to the rest of the Komsberg Suite. MORB and Chondrite normalization values after Sun and McDonough (1989) and Nakamura (1974), respectively. Average upper continental crust values from Taylor and McLennan (1985).*

Table 1. The average whole rock major trace element geochemistry for 11 Naros Granite samples compared with 74 analyses of other samples of the Komsberg Suite.

	Naros Granite			**Komsberg Suite**		
	Major Elements Wt %			**Major Elements Wt %**		
	mean ± 1σ	**max**	**min**	**mean ± 1σ**	**max**	**min**
	11 samples			**74 samples**		
SiO_2	67.64 ± 1.91	72.08	65.67	63.93 ± 4.47	72.08	47.28
TiO_2	0.93 ± 0.25	1.15	0.44	1.17 ± 0.41	3.24	0.37
Al_2O_3	13.32 ± 0.26	13.73	12.87	14.46 ± 1.47	24.28	12.47
Fe_2O_3 (t)	5.88 ± 1.40	7.04	2.73	7.27 ± 2.04	15.02	2.73
MnO	0.08 ± 0.03	0.11	0.02	0.10 ± 0.05	0.44	0.02
MgO	0.93 ± 0.26	1.16	0.41	1.75 ± 1.09	6.40	0.41
CaO	2.70 ± 0.56	3.25	1.54	3.58 ± 1.63	11.61	1.27
Na_2O	2.38 ± 0.26	2.74	1.92	2.35 ± 0.24	2.89	1.53
K_2O	4.96 ± 0.46	6.09	4.41	4.27 ± 1.06	6.71	0.74
P_2O_5	0.35 ± 0.11	0.47	0.10	0.35 ± 0.12	0.69	0.10
Cr_2O_3	0.01 ± 0.00	0.01	0.00	0.01 ± 0.01	0.05	0.00

	Naros Granite			**Komsberg Suite**		
	Trace Elements ppm			**Trace Elements ppm**		
	mean ± 1σ	**max**	**min**	**mean ± 1σ**	**max**	**min**
	7 samples			**74 samples**		
Li	27.6 ± 9.8	46.7	16.9	37.2 ± 16.2	104.8	13.5
Sc	12.5 ± 1.2	13.5	11.1	14.0 ± 4.9	26.7	6.8
V	63.3 ± 13.6	72.2	47.7	87.6 ± 51.1	301.1	16.2
Cr	9.9 ± 1.6	11.5	8.3	40.8 ± 53.9	303.3	3.8
Co	7.8 ± 0.8	8.4	6.9	12.7 ± 7.9	40.2	5.1
Cu	16.7 ± 2.2	18.1	14.2	19.1 ± 6.2	32.2	7.2
Zn	121.3 ± 28.3	153.3	99.4	112.4 ± 29.7	179.7	45.1
Rb	264.6 ± 38.9	292.4	220.2	195.5 ± 72.2	348.5	35.1
Sr	137.4 ± 43.1	181.2	95.0	190.7 ± 70.2	376.1	78.6
Y	63.3 ± 6.2	70.2	58.1	47.6 ± 15.0	71.8	17.4
Zr	234.7 ± 127.3	380.3	144.1	175.2 ± 90.5	418.9	26.2
Nb	27.0 ± 2.8	30.1	24.7	23.5 ± 7.8	44.0	8.4
Ba	1003 ± 194	1224	864	924.9 ± 225	1429.0	455.4
La	94.5 ± 13.2	109.6	85.5	85.5 ± 24.6	135.5	30.0
Ce	209 ± 26	239	190	186.0 ± 53.4	318.0	64.5
Pr	23.4 ± 2.2	25.7	21.4	21.3 ± 5.5	34.1	7.8
Nd	88.5 ± 6.7	92.9	80.7	80.8 ± 20.6	126.6	32.0
Sm	16.5 ± 1.6	17.9	14.8	14.7 ± 3.8	22.1	5.8
Eu	2.3 ± 0.3	2.6	2.1	2.3 ± 0.7	4.6	1.2
Tb	2.1 ± 0.1	2.2	1.9	1.7 ± 0.5	2.5	0.6
Gd	14.4 ± 1.1	15.4	13.3	11.9 ± 3.4	18.3	4.4
Dy	12.4 ± 0.9	13.3	11.6	9.7 ± 3.0	15.1	3.6
Ho	2.4 ± 0.2	2.6	2.2	1.9 ± 0.6	2.9	0.7
Er	6.8 ± 0.6	7.5	6.3	5.1 ± 1.7	8.1	1.9
Tm	1.0 ± 0.1	1.1	0.9	0.7 ± 0.2	1.2	0.3
Yb	6.2 ± 0.7	7.0	5.6	4.5 ± 1.6	7.4	1.7
Lu	0.9 ± 0.1	1.1	0.8	0.7 ± 0.2	1.1	0.3
Hf	6.6 ± 3.3	10.4	4.2	4.9 ± 2.3	11.5	1.1
Ta	1.7 ± 0.3	2.0	1.5	1.4 ± 0.4	2.6	0.6
Pb	34.9 ± 1.3	36.3	33.9	29.1 ± 7.6	43.7	8.8
Th	33.4 ± 7.0	38.0	25.4	25.1 ± 13.3	73.1	2.2
U	4.3 ± 0.6	4.9	3.7	2.8 ± 1.4	6.0	0.4
Ga	21.8 ± 0.2	22.0	21.7	31.0 ± 14.0	66.0	18.2

Table 2. Sm-Nd isotope data for two samples of Naros Granite.

Sample Number	Latitude	Longitude	Sm ppm	Nd ppm	$^{147}Sm/^{144}Nd$ Calculated	$^{143}Nd/^{144}Nd$ Measured	±2s internal	εNd	T_{DM} (in MA)
PM14072	28°32'12"S	19°31'39"E	14.81	80.73	0.110890	0.511999	11	-0.28	1579
RT14/01	28°38'59"S	19°29'9"E	16.77	92.86	0.109163	0.511987	13	-0.26	1570

other granitoids of the Komsberg Suite (Macey et al., 2015; Figure 9b) but with higher HREE/LREE than the rest of the suite.

The Naros Granite is the youngest and most evolved member of the Komsberg Suite in the Lower Orange River area. The unit has the highest average SiO_2 and total REE, high K_2O and Rb and low CaO and Sr and has elevated concentrations of incompatible elements relative to the rest of the suite. Two samples of Naros Granite yielded near identical εNd values of -0.28 and -0.26 and T_{DM} model ages of 1570 and 1579 Ma (Table 2) which is typical for the Komsberg Suite (Macey et al., 2015, 2018) and points to significant contribution of older, probably Palaeoproterozoic, crust in the Naros Granite magma.

The majority of the Komsberg Suite granitoids, including the Naros Granite show regular inter-element variations, are hornblende- and sometime orthopyroxene-bearing, do not contain muscovite or alumina silicate phases and have abundant mafic autoliths. This points to an I-type granite parentage (Chappell and White, 1974) and were likely produced by partial melting of older igneous rocks that had not undergone significant chemical weathering.

Acknowledgements

We thank S. Büttner and R. Bailie for their constructive reviews of earlier versions of the manuscript.

References

Abrahams, Y. and Macey, P.H., 2020. Lithostratigraphy of the Mesoproterozoic Donkieboud Granodiorite Granite. South African Journal of Geology. 123, 421-430.

Bailie, R., Macey, P.H., Nethenzheni, S., Frei, D. and le Roux, P., 2017. The geochronology and geochemistry of the ferroan granites on the eastern margin of the Namaqua Metamorphic Province, southern Africa: The Keimoes Suite of the 1.2-1.07 Ga Namaquan Orogeny revisited. Journal of African Earth Science, 134, 737-765.

Bial, J., Büttner, S.H. and Frei, D., 2015. Formation and emplacement of two contrasting late-Mesoproterozoic magma types in the central Namaqua Metamorphic Complex (South Africa, Namibia): evidence from geochemistry and geochronology. Lithos 224-225, 272-294.

Chappell, B.W., and White, A.J.R., 1974. Two contrasting granite types. Pacific Geology, 8, 173-4.

Chayes, F., 1985. IGBADAT: a world database for igneous petrology. Episodes, 8, 245-251.

Cornell, D.H., Thomas, R.J., Moen, H.F.G., Reid, D.L., Moore, J.M. and Gibson, R.L. 2006. The Namaqua-Natal Province. In: M.R. Johnson, C.R. Anhaeusser and R.J. Thomas (Editors), The Geology of South Africa. Geol. Soc. S. Afr., Johannesburg/Council for Geoscience, Pretoria, 325-379.

Cornell, D.H., Pettersson and Å. and Simonsen, S.L. 2012. Zircon U-Pb emplacement and Nd-Hf crustal residence ages of the Straussburg Granite and Friersdale Charnockite in the Namaqua-Natal Province, South Africa. South African Journal of Geology, 115, 465-484.

Cox, K.G., Bell, J.D. and Pankhurst, R.J., 1979. The interpretation of igneous rocks. George Allen and Unwin Ltd, London, 450pp.

Doggart, S., Macey, P.H. and Frei, D., 2021. Lithostratigraphy of the Mesoproterozoic Twakputs Gneiss. South African Journal of Geology. 124, 783-794

Du Plessis, G., 1979. 'n Metamorf-magmatiese studie van 'n deel van die Namakwalandse Metamorfe Kompleks langs die Oranjerivier oos van Onseepkans. M.Sc. Thesis, University of the Orange Free State, Bloemfontein, 139p.

Du Plessis, G., 1986. 'n Petrochemiese ondersoek van die graniete van die Namakwalandse Metamorfe Kompleks langs die Oranjerivier oos van Onseepkans. PhD. Thesis, University of the Orange Free State, Bloemfontein, 274p.

Groenewald, C.A. and Macey, P.H., 2020., Lithostratigraphy of the Mesoproterozoic Yas-Schuitdrift Batholith. South African Journal of Geology. 123, 431-440.

Macey, P.H., Minnaar, H., Miller, J.A., Lambert, C., Kisters, A.F.M., Diener, J., Thomas, R.J., Groenewald, C., Indongo, J., Angombe, M., Smith, H., Shifotoka, G., Le Roux, P. and Frei, D., 2015. The Precambrian geology of the Warmbad region, southern Namibia. Interim explanation to the Precambrian geology 2818 Warmbad sheet accompanied by twenty-four 1:50 000 geological maps. Geological Survey of Namibia. Council for Geoscience South Africa.

Macey, P.H., Abrahams, Y and Miller, J.A. 2018. Lithostratigraphy of the Mesoproterozoic Stolzenfels Enderbite (Komsberg Suite), South Africa and Namibia. South African Journal of Geology,121, 217-226.

Moen, H.F.G., 1988. 1:250 000 scale Geological map sheet 2820 Upington, Geological Survey of South Africa/Council for Geoscience.

Moen, H.F.G. and Toogood, D.J., 2007. The geology of the Onseepkans area. Map and explanation, sheet 2818 Onseepkans (1:250 000), Council for Geoscience, Pretoria, 101pp.

Nakamura, N., 1974. Determination of REE, Ba, Fe, Mg, Na and K in carbonaceous and ordinary chondrites. Geochimica et Cosmochimica Acta 38, 757-775.

Shand, S.J., 1943. Eruptive Rocks. Their genesis, composition, classification, and their relation to ore-deposits with a chapter on meteorite. New York: John Wiley and Sons.

Smith, H.P. and Macey, P.H., 2018. 2819CB 1:50 000 Geological Map of Onseepkans, Council for Geoscience.

Streckeisen, A.L. and le Maitre, R.W., 1979. A chemical approximation to the modal QAPF classification of the igneous rocks. Neues Jahrbuch Mineralogie, Abhandlungen, 136, 169-206.

Sun, S.S. and McDonough, W.F., 1989. Chemical and isotopic systematics of oceanic basalts: implications for mantle composition and processes. In: A.D Saunders and M.J. Norry (Editors), Magmatism in ocean basins. Geological Society London. Special Publication, 42, 313-345.

Taylor, S.R. and McLennan, S.M., 1985. The continental crust: Its composition and evolution. Blackwell, Oxford, 312pp.

Toogood, D.J. 1976. Structural and metamorphic evolution of a gneiss terrain in the Namaqua Belt near Onseepkans, South West Africa. Bulletin, Precambrian Research Unit, University of Cape Town, 19, 220pp.

Editorial handling: C.R. Penn-Clarke.